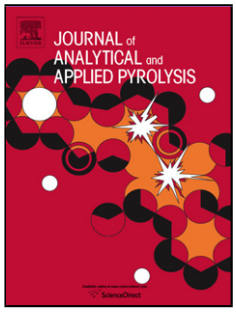

Title: Chemical properties of biosilica and bio-oil derived from fast pyrolysis of *Melosira varians*

Authors: Roxana V. Piloni, Verónica Brunetti, R. Carlos Urcelay, I. Claudia Daga, E. Laura Moyano

PII: S0165-2370(17)30121-3
DOI: http://dx.doi.org/doi:10.1016/j.jaap.2017.07.009
Reference: JAAP 4087

To appear in: *J. Anal. Appl. Pyrolysis*

Received date: 30-1-2017
Revised date: 12-6-2017
Accepted date: 17-7-2017

Please cite this article as: Roxana V.Piloni, Verónica Brunetti, R.Carlos Urcelay, I.Claudia Daga, E.Laura Moyano, Chemical properties of biosilica and bio-oil derived from fast pyrolysis of Melosira varians, Journal of Analytical and Applied Pyrolysishttp://dx.doi.org/10.1016/j.jaap.2017.07.009

Chemical properties of biosilica and bio-oil derived from fast pyrolysis of *Melosira varians*

Roxana V. Piloni,[a] Verónica Brunetti,[b] R. Carlos Urcelay,[c] I. Claudia Daga,[c] E. Laura Moyano[a]

[a]INFIQC (CONICET-Universidad Nacional de Córdoba), Departamento de Química Orgánica, Facultad de Ciencias Químicas, Córdoba, Argentina.

[b]INFIQC (CONICET-Universidad Nacional de Córdoba), Departamento de Fisicoquímica, Facultad de Ciencias Químicas, Córdoba, Argentina.

[c]IMBIV (CONICET - Universidad Nacional de Córdoba), Facultad de Ciencias Exactas, Físicas y Naturales, Córdoba, Argentina.

***Corresponding Author,** E-mail: lauramoy@fcq.unc.edu.ar (E. L. Moyano), Phone: +54 351 5353867

Highlights

- Fast pyrolysis of diatom *Melosira varians* generate high yields of biosilica
- Bio-oil produced at 400-500 °C is mainly composed by fatty acids as palmitic and myristic acids
- Capacitive properties of diatom solids are poor but its composites with CNT substantially improved the electrochemical performance

ABSTRACT

This study examined bio-oil and solid products generated from the diatom *Melosira varians* by fast pyrolysis using a fixed-bed reactor with inert gas flow and a vacuum

medium. The effect of temperature (300-700 ºC) on product yields, the bio-oil composition and the properties of the solid fraction were evaluated. It was found that the most suitable temperature to obtain significant amounts of high-quality bio-oil (29 % yield) was 450 ºC, at which point fatty acids appeared as main components. Under all operating conditions a solid material, mainly composed of siliceous frustules, was the most abundant product (59-88 % yield). These materials were exhaustively characterized by SEM microscopy, Raman and FT-IR spectroscopy, XRD, elemental analysis and BET surface analyses. The structure and morphology of the biosilica were practically unaltered in the studied temperature range. The conductivity properties of the solids derived from diatom and their composites with carbon nanotubes were determined using cyclic voltammetry.

Keywords**:** Diatom; Fast pyrolysis; Biosilica; Biomass; Microalgae

1. Introduction

In an effort to meet the challenge of diminishing fossil resources, the use of biomass for the production of bioenergy and biomaterials has grown rapidly over the last decade [1]. Biomass is the material derived from living or recently living organisms such as plants, animals and their byproducts, and has the advantage that it is a renewable raw material, is biodegradable, consists for the most part of organic waste matter and is environmentally friendly.

After appropriate treatment, several products can be obtained from biomass: bio-oil, biodiesel, carbonaceous materials, siliceous materials, bioactive compounds, functional foods and nutraceuticals, among others. In this context, algae emerge as an interesting source of biomass in view of their rapid growth rate and high photosynthetic efficiency; algae do not require large tracts of land or clean water for cultivation, and most importantly, they do not compete for fertile, productive agricultural land or interact with established food or feed commodity markets [2]. In particular, diatoms are unicellular, sometimes colonial algae, found in almost every aquatic habitat as free-living photosynthetic autotrophs [3,4]. Diatoms are therefore considered to be promising feedstock for application in functional food, pharmaceutical and fuel industries, as biomolecules and for bioremediation, among others.

Diatoms are microalgae which create a wide variety of three-dimensional amorphous silica shells [5]. These rigid cell walls, the so-called frustules, consist of assembled silica nanoparticles with a high degree of organization and multiple pore arrangements usually at the micrometric scale. They possess other unique properties such as thermostability, excellent absorption capacity, chemical inertness, and a relatively low price [6], all of which favor their use as filter aids, adsorbent, insulating material, catalyst support or carrier, natural insecticide, drug delivery devices, etc. [7,9]. Although diatom biosilica has attracted wide interest, research into and applications of biosilica are still in their infancy, considering the tremendous variety in their shapes and substructures. These siliceous materials are also found in diatomite or diatomaceous earth, a non-metallic mineral composed of the skeletal remains of diatom algae, found

mostly on the bottom of oceans and lakes [10,11]. The recovery of diatomite deposits by mining and their processing involves considerable cost.

The aim of our paper was to study an alternative, less expensive and faster way to obtain a biosilica-like structure without destroying the environment, which led us to the application of fast pyrolysis for the treatment of diatom algae as a preparation method for siliceous materials. Pyrolysis, the thermal decomposition of organic material in the absence of oxygen, has been investigated as a practical route for the generation of renewable fuels and chemicals from biomass [12]. The three main products obtained are: a solid product, sometimes called bio-char, a liquid fraction (bio-liquid) and non-condensable gases (bio-gas). The relative proportion of these products is influenced by feedstock properties and operation parameters such as temperature, heating rate, particle size, vapor residence time, etc. [1,12]. A lower processing temperature and longer vapor residence times favor the solid fraction (slow pyrolysis or carbonization), high temperatures and longer residence times increase the biomass conversion to gas (gasification) and moderate temperature and short vapor residence times are optimum for producing liquids (fast pyrolysis) [12]. The addition of vacuum media in the pyrolysis experiment enhances the volatilization and internal diffusion of products in the pyrolysis process, which contributes to attenuating the secondary reactions of the repolymerization and carbonization of these products on the surface of the char [13].

Here, the fast pyrolysis of the diatom *Melosira varians* C. Argadh in a vacuum media was studied as an alternative chemical process to obtain biosilica. The feasibility of using this pyrolytic solid for electrode materials, studying the relationship between the

solid properties and its performance as capacitor, was explored using the cyclic voltammetry technique, in a 1 M H_2SO_4 electrolyte.

2. Materials and methods

2.1. Materials

The raw material in this research was *Melosira varians* (MV), a cosmopolitan freshwater alga. The material was collected in the slow-flowing stream Arroyo Cabana (31° 11' 44" S; 64° 21' 58") in the central region of Argentina.

After collection, the mats of MV filaments were processed in the laboratory: they were first washed under running water using a mesh of 1 mm in order to keep the mats and remove unicellular organisms, followed by the removal of less abundant filamentous algae using a binocular stereoscope. The remaining material was air dried at room temperature and characterized before the pyrolysis experiments by elemental analysis, Raman spectroscopy, FT-IR spectroscopy, SEM, BET surface area and XRD with the equipment described below.

All organic solvents used in this study were analytical grade and used without further purification. H_2SO_4 for electrochemical experiments was reagent grade and was

used without further purification. Electrolyte solutions were prepared immediately prior to their use and water was purified with a Millipore Milli-Q system.

The carbon nanotubes (CNT) employed in this work were supplied by Sunnano, China. The nanotubes were synthesized by chemical vapor deposition (CVD) and have around 80% of purity. The diameter ranged between 10 and 30 nm.

2.2. Pyrolysis experiments

The fast pyrolysis reactions were conducted in a batch cylindrical quartz reactor under inert atmosphere. The reactor with a length of 25.00 cm and an inner diameter of 2.50 cm was heated externally by using a tube furnace with a temperature-controller device. The reactor was connected to a high vacuum pump where pressures were in the range of 0.01-0.05 Torr and a flow of oxygen-free dry nitrogen permanently circulated inside the reactor at rates of 0.1 $mL.s^{-1}$. Nitrogen as inert carrier gas improves the transportation of products form the pyrolysis region to the condensation trap. Liquid products were trapped at liquid nitrogen temperature (- 196 ºC) immediately after their escape from the hot zone. In a typical experiment an algal sample (0.20 g) was placed in a sliding ceramic boat, which was fed into the pyrolysis furnace when temperature and vacuum conditions were reached. The sample was subjected to pyrolysis conditions for 40 min and contact times were very short (< 0.1 s) due to the vacuum system. This pyrolysate was extracted with acetone from the condensation trap and subjected to GC-MS analyses. After evaporation of organic solvent, the liquid phase was weighed. The

solid material was removed from the ceramic boat and weighed after which the gas yield was calculated by difference.

2.3. Characterization techniques

The raw algal material and the solid produced in the pyrolysis reactions were exhaustively characterized by elemental analysis, Raman spectroscopy, FT-IR, XRD, SEM, EDS and BET.

Elemental analyses of the samples were performed in a CHNS Elemental Analyzer 2400 Serie II Perkin Elmer.

For the Raman measurements, a spectrometer Horiba-JobinYvon (INFIQC, UNC) coupled with a confocal microscope was used. The spectra were recorded with Ar laser radiation (514.53 nm), with a power of 2.81 mW and the observation of the surface was carried out with different objectives, changing the magnification.

FT-IR spectra were measured by an IR NICOLET AVATAR-360 spectrophotometer at room temperature using KBr tablets.

X-Ray diffraction patterns were recorded in a Panalytical X'Pert Pro instrument (40 mV, 40 mA), using a Cu Kα (λ = 1.5418 Å) radiation and graphite monochromator. The data were collected in the 2θ range: 9.01313-79.99544° and the scanning step was 0.026°, with a scan step time of 2 seconds per point.

The topography of the pyrolyzed samples was determined by an *in-lens* detector in the Field Emission Scanning Electron Microscopy (FE-SEM Σigma, Carl Zeiss) at 10 kV. The samples were previously metalized with a 20 nm-layer of Au.

The chemical composition analysis was performed by energy dispersive X-ray spectroscopy (EDS, Oxford). SEM and EDS studies were carried out in LAMARX (Laboratorio de Microscopía Electrónica y Análisis por Rayos X) from FAMAF (Facultad de Matemática, Astronomía y Física) at the National University of Córdoba.

Measurements of surface area were carried out using a Micromeritics Chemisorb 2700 (CITEQ-National Technological University). Determinations were made by placing the sample in a reservoir, degassing vacuum during 1 hour at 250 °C and measuring nitrogen adsorption by single-point definition using the Brunauer-Emmett-Teller (BET) method at the temperature of liquid nitrogen (77 K, - 196 °C).

GC-MS analyses of the bio-liquid obtained in the pyrolysis experiments were performed in a Shimadzu GC–MS-QP 5050 spectrometer. The injector temperature was kept at 300 ºC and the separation was performed using a VF-5ms capillary column. Helium was used as a carrier gas with a constant flow rate of 0.5-1.0 $\mu L.min^{-1}$. The oven temperature was programmed from 80 ºC (3 min) to 280 ºC (15 min) with a heating rate of 10 $^oC.min^{-1}$. The temperature of the GC-MS interface was held at 280 ºC and the mass spectrometer was operated at 70 eV under electron ionization. The liquid fraction was analyzed by GC-MS technique, where the peak area percentage of the detected products depends on the response factor of the mass spectrometer detector, rendering it difficult to accurately quantify the products. With this in mind, the peak area of an individual compound was considered to be directly proportional to the concentration of the compound in the liquid pyrolysate. Thus, the peak area percentage of a compound was used to compare the change in its relative amount in the bio-oil under the different conditions. The identification of chromatographic peaks corresponding to the different compounds was achieved according to NIST MS library (match > 85%).

2.4. Electrochemical experiments

The electrochemical properties of the solids were analyzed by cyclic voltammetry in 1 M H_2SO_4 solution using a multipurpose electrochemical analyzer from CH Instrument CHI760C (INFIQC, UNC). A conventional three-electrode cell was used containing an Ag/AgCl reference, a Pt counter electrode and glassy carbon as working electrode. Nitrogen gas was used to remove air from all aqueous solutions before their use. The values of capacitance were obtained as an average of three experiments.

The solid product obtained from pyrolysis was immobilized onto glassy carbon electrodes by double-sided conductive carbon tape (SPI Supplies®). The amount of immobilized powder was quantified by mass difference.

The preparation of MV-CNT composites was carried out by a mechanical mixture, at room temperature, of the dried solid obtained in diatom pyrolysis (350 ºC) and the commercial nanotube powder. Three ratios of components were used for the composites: CNT:MV equal to 80:20, 50:50 and 20:80 %wt.

3. Results and discussion

3.1. Fast pyrolysis of *Melosira varians*

The fast pyrolysis experiments of diatom *Melosira varians* (hereinafter referred to as MV) were performed between 300 and 700 ºC, giving liquid, solid and gas products. The percentages of these products at different temperatures are given in Figure 1.

At all temperatures, the solid fraction was predominant (59-88 % yield). It can be seen that an increase in temperature resulted in a greater amount of bio-liquid, obtaining

a maximum yield at 450 °C (29 %) at which point the yield began to decline and gaseous products became significant. Similar results were found in the thermal study of other micro- and macro-algae as outlined in the literature [14,16].

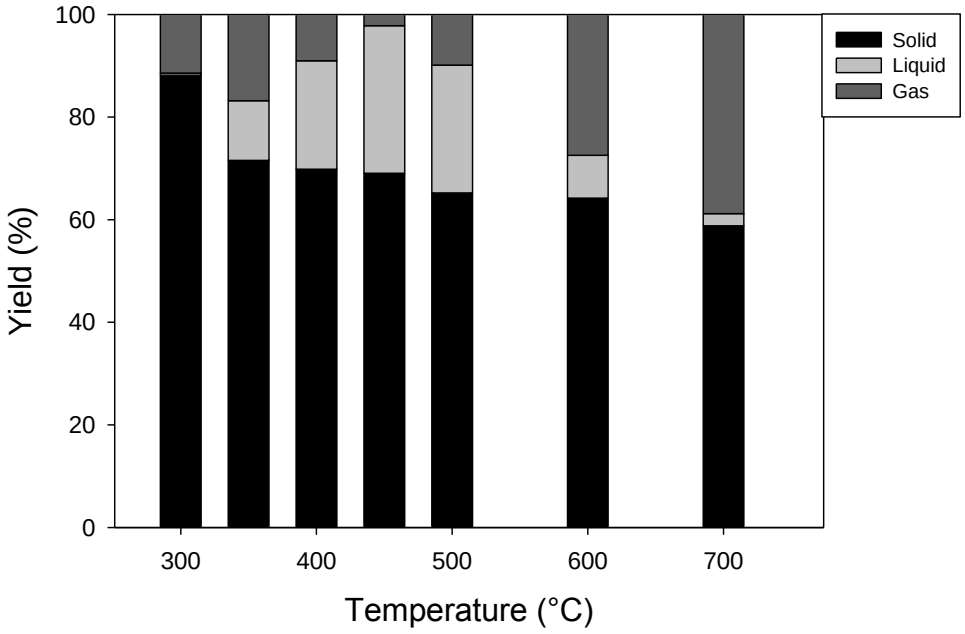

Figure 1. Product distribution at different pyrolysis temperatures

GC-MS analysis was carried out in order to determine the components of organic compounds in the bio-oil produced under optimum pyrolysis conditions (400, 450 and 500 ºC). Products were identified by the GC-MS software library and could be classified into four main groups: long chain acids (LCA), nitrogenated compounds (NC), anhydrosugars (ANH) and other oxygenated compounds (OC). The percentage area of these groups is shown in Figure 2.

In the first group, tetradecanoic (myristic) and hexadecanoic (palmitic) acids were the main components; palmitic acid in particular was formed in large amounts (80% of

the total LCA) at 400 ºC. These fatty acids have been reported in the degradation of many algae species [17], the actual amount decreasing with rises in temperature probably through fragmentation of these high molecular weight compounds into small ones.

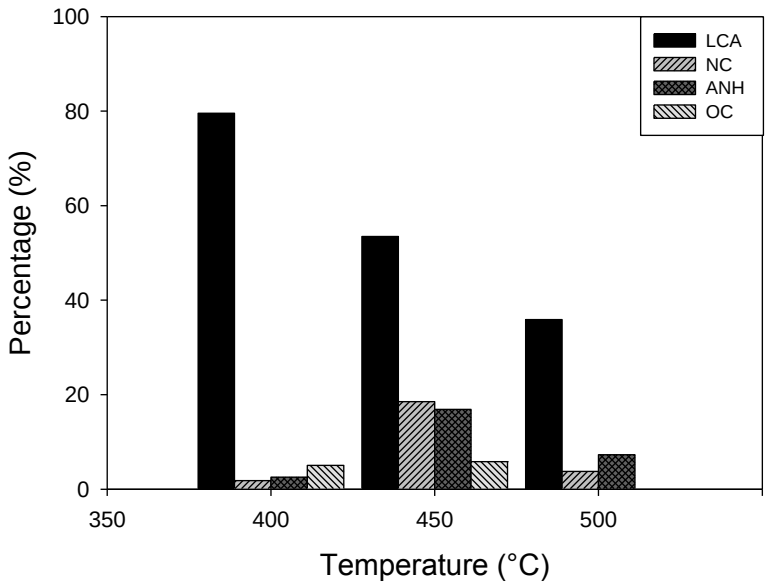

Figure 2. Composition of bio-oil at different temperatures. LCA: long chain acids, NC: nitrogenated compounds, ANH: anhydrosugars, OC: other oxygenated compounds.

The nitrogen-containing compounds in algal bio-oils, such as 4-amino-4-methyl-2-pentanone and xanthosine, were assumed to be derived from protein degradation. Though the formation of these compounds was favoured at 450 °C, they were present at all three studied temperatures. The high nitrogen content presents a challenge in using these bio-oils as fuels, calling for some further de-nitrogenation process. Nevertheless, there is scope for the production of useful chemical commodities.

Anhydrosugars levoglucosan (LG) and 1,4:3,6-dianhydro-α-*d*-glucopyranose (DGP) were clearly identified in appreciable amounts in the mixture at 450 ºC. These compounds are produced by the depolymerization reaction of the cellulose present in the raw algae. LG is an interesting precursor of platform chemicals and chiral natural products [18,19] and is often used as a highly specific tracer for biomass burning aerosols [19,20]. DGP is proposed to be an intermediate in the dehydration of LG to form levoglucosenone (LGO), another valuable anhydrosugar [19]. Under the reaction conditions studied here, LGO was not detected in the bio-oils derived from MV.

The last group, termed other oxygenated compounds, includes phenols, ethers and ketones that could be formed from the different constituents (proteins, cellulosics) of the starting algal material. A slight increment was visualized at 450 ºC, but the compounds were not detected at 500 ºC.

Although the bio-oil yield was not very high, the presence of large amounts of fatty acids confer high value on this liquid, which after appropriate upgrading can be improved and converted into an attractive biofuel.

3.2. Characterization of raw algae and pyrolytic solid products

Unlike other types of algae, the diatom MV presents low carbon and nitrogen content (Table 1) [9,21]. However, the nitrogen content is quite high compared to lignocellulosic biomass such as sugar cane bagasse (0.5 %), corn cob (0.3 %) and corn stover (0.6 %) [22].

A primary visual analysis of the solid obtained after pyrolysis reactions of MV revealed variations in color depending on the pyrolysis temperature (see SI). Thus, at

300 °C the solid was black and this colour was attenuated with increasing temperatures until the obtention of a pinkish white material, indicating that the carbon content decreased with rises in temperature, as confirmed in the final analysis of solids (Table 1). As a point of practicality, we named as MV-300, MV-350, MV-400, MV-450, MV-500, MV-600 and MV-700 the solids obtained from pyrolysis of *Melosira varians* at 300, 350, 400, 450, 500, 600 and 700 ºC, respectively.

Table 1. - Elemental analysis of raw algae and solid products from pyrolysis

Sample	T (ºC)	% C[a]	% H[a]	% N[a]
MV	-	10.23	1.12	1.27
MV-300	300	4.85	0.59	0.71
MV-350	350	3.23	0.11	0.43
MV-400	400	2.14	0.05	0.26
MV-450	450	2.14	0.06	0.19
MV-500	500	1.56	0.02	0.01
MV-600	600	0.50	0.03	0.04
MV-700	700	0.67	-	0.03

[a]Determined on dry basis.

It can be seen that the carbon content of all samples was very low, so the elevated solid percentage obtained from the diatom pyrolysis did not correspond to a product with

biochar features. This finding was the first indicator that siliceous frustule components make up most of the weight of algae.

Raman spectroscopy of the raw algae and solid products exhibited two broad and strongly overlapping peaks with maximum intensity at ~1350 cm^{-1} and ~1580 cm^{-1}, associated with the graphitic bands D and G, respectively (see Figure 3). The G band corresponds to an ideal graphitic lattice vibration mode, and the D band is known to be characteristic for disordered graphite [3,23]. As the pyrolysis temperature increased, these two bands diminished until they disappeared completely in the solid obtained at 500 °C onwards. This behavior is also an indication that the carbon content falls as the temperature rises, which correlates with the observations made above.

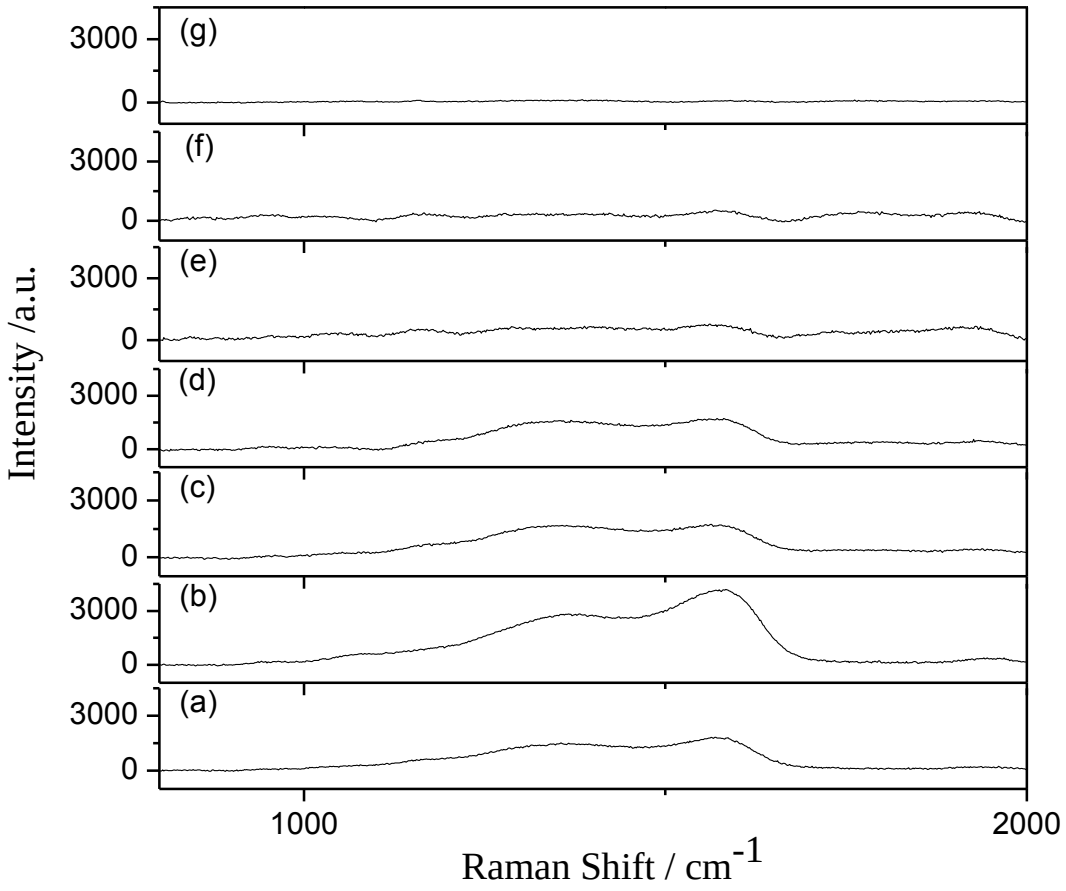

Figure 3. Raman spectra of different solid materials: (a) starting MV, (b) MV-300, (c) MV-350, (d) MV-400, (e) MV-500, (f) MV-600 and (g) MV-700.

FT-IR spectra of feedstock and the products from pyrolysis are presented in Figure 4. Different spectra reflect changes in the surface functional groups of materials produced at different temperatures. Spectroscopic assignments indicate bands due to the O-H stretching of water and Si-OH (~3415 cm^{-1}), Csp^3-H stretching (~2930 and ~2850 cm^{-1}), other bands associated with H_2O bending (~1630 cm^{-1}) and an intense band related with Si-O-Si stretching (~1090 cm^{-1}), inter-tetrahedral Si-O-Si bending

(~798 cm^{-1}) and O-Si-O bending (~465 cm^{-1}) [24,25]. These findings show that a high concentration of an important part of the solids corresponded to siliceous materials from the original diatom silica frustules [25]. In the spectra comparison, it could be observed that the starting alga sample showed intense bands attributed to the presence of absorbed water and organic components (see Figure 4). These bands practically disappeared in the material after pyrolysis processes. Likewise, the signals associated with the silicate structure did not change along the temperature variation. These findings point to the higher degree of purity of the biosilica material produced at elevated temperatures.

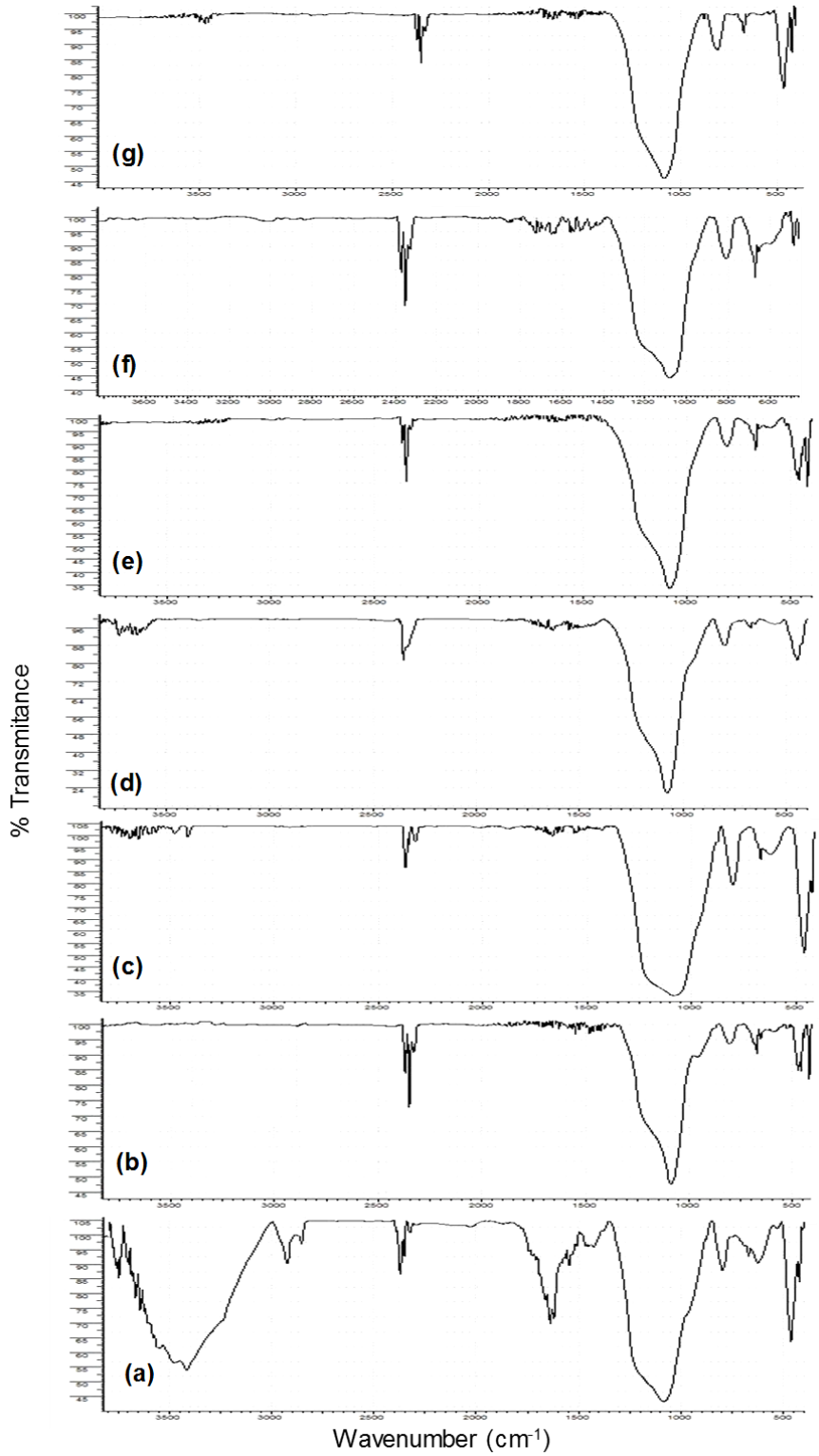

Figure 4. Comparative FT-IR spectra: (a) starting diatom MV, (b) MV-300, (c) MV-350, (d) MV-400, (e) MV-500, (f) MV-600 and (g) MV-700.

The X-ray diffraction analysis of the pyrolyzed diatom samples is shown in Figure 5. The XRD patterns show an opal structure (tagged as O), which is hexagonal silica, with quartz (tagged as Q), confirming that the samples consisted of predominantly amorphous silica [26]. At 700 ºC, the XRD pattern exhibits more pronounced and thin peaks indicating a slight increment in crystallinity.

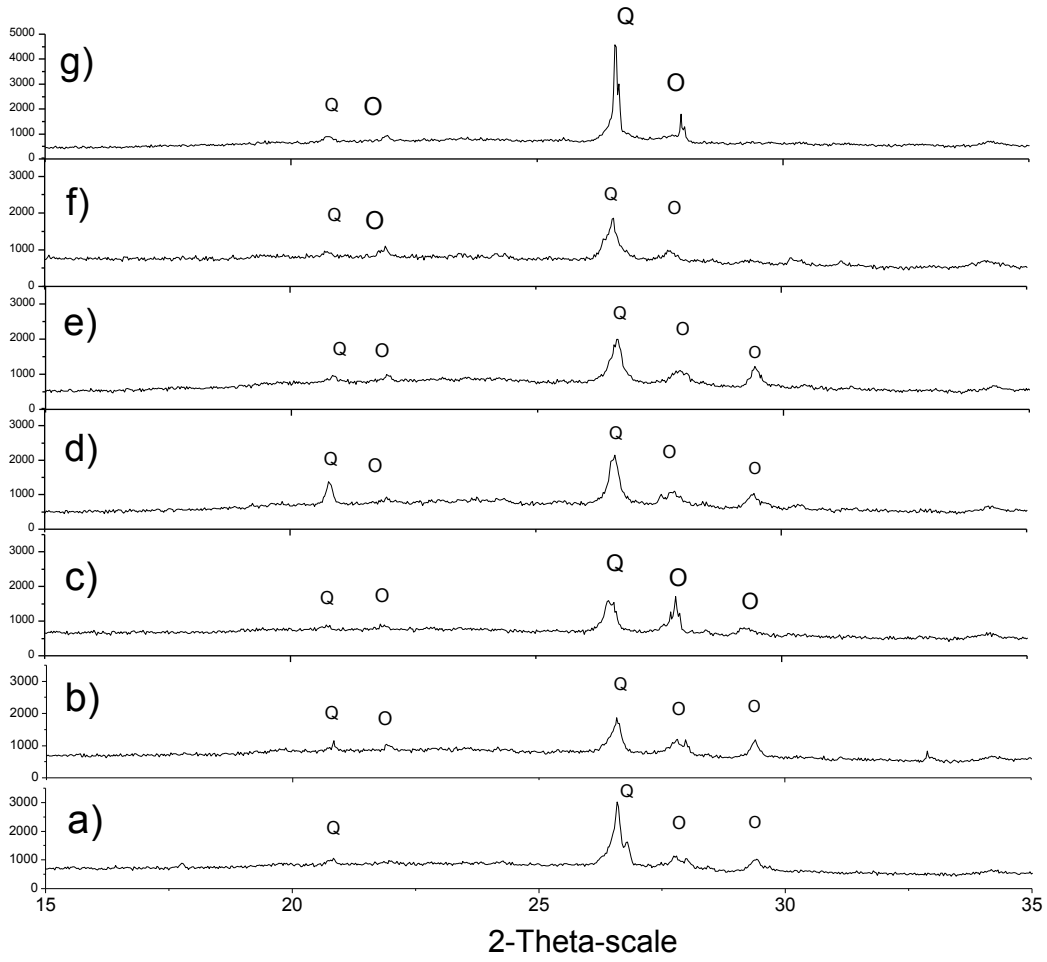

Figure 5. XRD patterns of alga samples: (a) MV-300, (b) MV-350, (c) MV-400, (d) MV-450, (e) MV-500, (f) MV-600 and (g) MV-700.

The morphology of the different solid materials was observed by SEM. All the evaluated samples exhibited a cylindrical shape, a common feature of diatom frustules, with a length between 40 and 50 µm, and a diameter between 10 and 15 µm, represented in Figures 6a and 6b for the samples of diatom after pyrolysis at 300 ºC (MV-300). The SEM images at high magnification show high porosity, but with very small pores, approximately 20-30 nm in size (see Figure 6c and 6d). These diatom biosilica micro- and nanostructures are well known and have attracted the interest of researchers owing to their extraordinary material properties [3,20,21]. The micrographs of samples obtained at high pyrolysis temperatures show that thermal treatments did not greatly affect the morphology of the biosilica (see Figure 7). It was also noted that all the samples exhibited a minor amount of other varieties of algae and impurities.

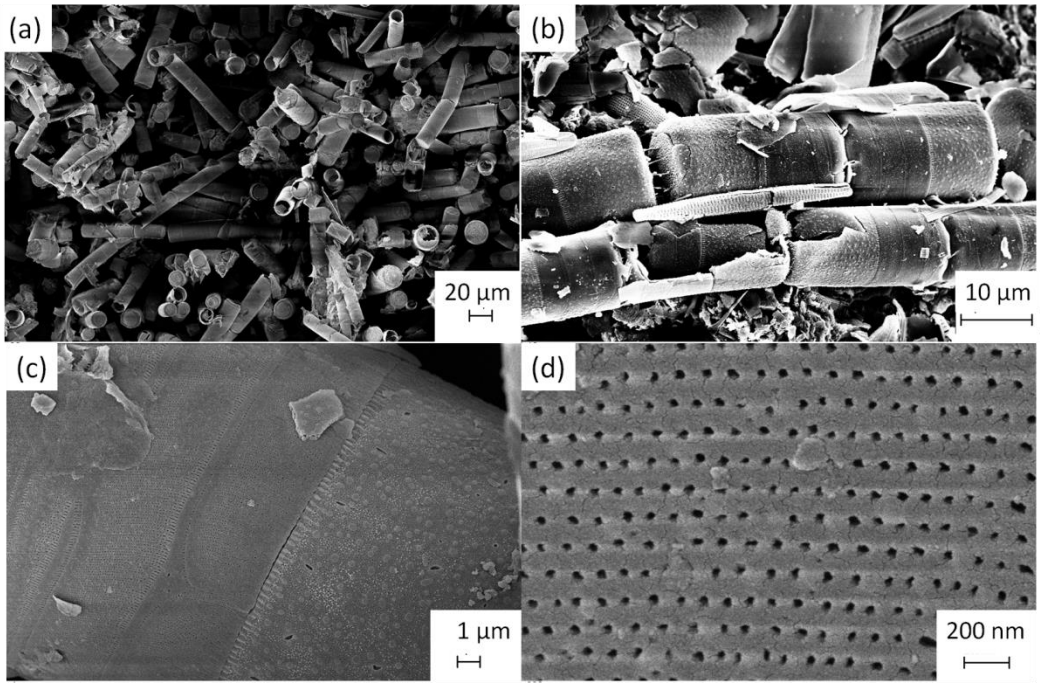

Figure 6. SEM micrographs of MV-300 at different magnifications

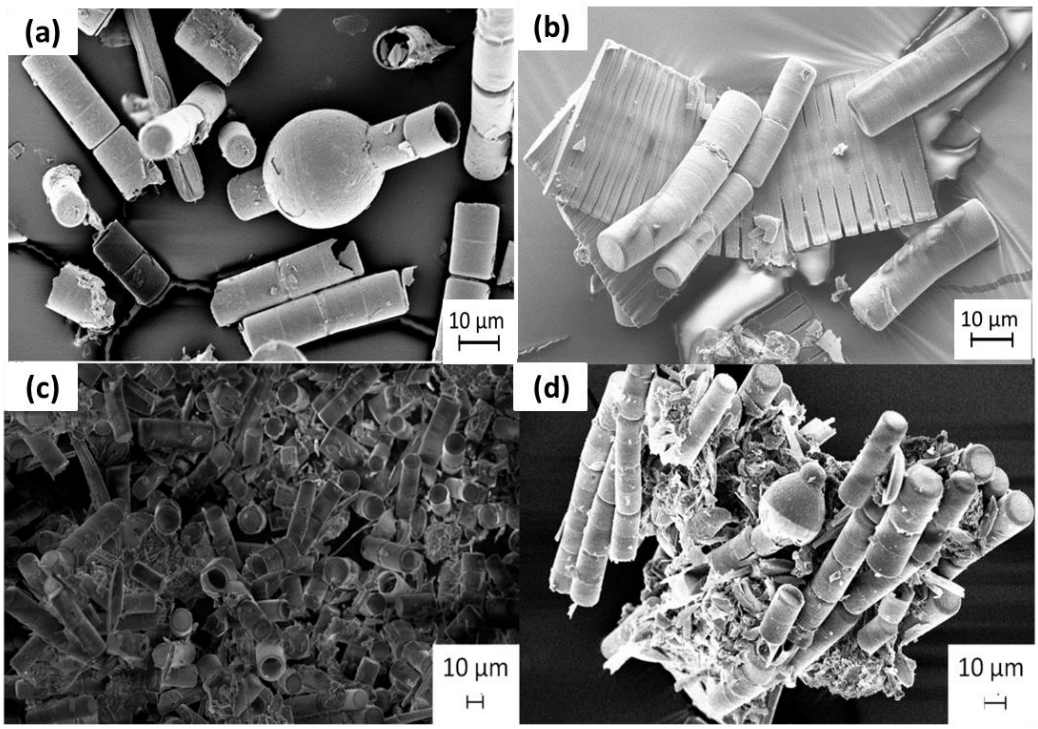

Figure 7. SEM micrographs of diatom samples: (a) raw MV, (b) MV-450, (c) MV-600, and (d) MV-700.

EDS used in the semi-quantitative mode to determine chemical composition by peak-height ratio relative to a standard (see the graphics in SI) showed an important percentage of oxygen and silicon (see Table 2), coinciding with the silica composition of the frustules. Furthermore, it was observed that the relative amount of Si in the untreated sample and in the solid pyrolysis products remained almost constant, whereas the carbon content decreased with increasing pyrolysis temperatures, compared with the raw material.

According to the literature, biosilica arising from diatoms displays low specific surface areas. The values obtained from the BET model differ among species and range from 2 $m^2.g^{-1}$ to 39 $m^2.g^{-1}$ [3,9,27]. Moreover, similar BET surface areas were reported

for diatomite and diatomaceous earth, taking into account that a mix of diatom species is found in these cases [28,29]. Table 3 summarizes the BET surface area values for the siliceous solids generated in the fast pyrolysis of MV. A slight increase in area can be seen in the material produced at 350 ºC; however, there was no meaningful change with respect to the starting alga.

Table 2. Elemental composition determined by the SEM-EDS technique

Sample	% O	% Si	% C	% Ca	% K
MV	37	40	22	1	-
MV-300	49	38	12	1	-
MV-350	53	35	9	1	2
MV-400	56	34	9	1	-
MV-450	45	47	7	1	-
MV-500	44	44	10	1	1
MV-600	55	40	4	1	-
MV-700	58	36	5	1	-

Table 3. The BET specific surface area of diatom solids

Sample	MV	MV-300	MV-350	MV-400	MV-450	MV-500	MV-600	MV-700
S_{BET} ($m^2.g^{-1}$)	14	15	21	13	17	17	15	12

3.3 Capacitance properties of pyrolytic solids

The solid materials generated in the pyrolysis of MV were used to modify glassy carbon electrodes and their capacitance was evaluated by voltammetric profiles obtained at different scan rates [30]. Table 4 shows the specific capacitance values of samples obtained at the different pyrolysis temperatures. The specific capacitance of the materials decreased with rising temperatures up to 500 and 600 ºC, after which the values deviated slightly from this trend. At 700 ºC the specific capacity value decreased again. This behavior could not be attributed to any single feature of the algal materials but rather a combination of factors including the polydispersibility of the solids that affect the active area of the electrodes. Furthermore, the capacitance values were very low compared to materials from other algae: in the case of *T. turbinate* the solids displayed capacities of 8-74 $F.g^{-1}$, depending on the pyrolysis temperature [31]; for *E. prolifera* [32] capacities ranged from 100 to 296 $F.g^{-1}$; and for solids generated from *L. nigrescens* capacities were high, in the range from 125 to 255 $F.g^{-1}$, depending on the electrolyte [33]. The lower values observed for diatom-derived materials could be caused by low BET surface areas, low carbon content and the predominance of biosilica structures.

Table 4. Specific capacitance values of diatom samples

Sample	MV-300	MV-350	MV-400	MV-450	MV-500	MV-600	MV-700
Csp ($F.g^{-1}10^{-3}$)	6.5	4.4	2.7	1.6	3.6	3.5	1.5

It is widely known that carbon nanotubes (CNT) can efficiently improve the capacitance of some surfaces owing to an increase in the area exposed to the electrolyte

[34-36]. Thus, the capacitance of composites formed by CNT and the siliceous samples derived from MW pyrolysis was explored. Table 5 shows the specific capacitance values of these new nanocomposites containing CNT and MV-350 in different mixing ratios and in Table 6 the specific capacitance values of nanocomposites CNT:MV (80:20) formed by the bio-silica samples obtained for all the evaluated temperatures.

Table 5. Specific capacitance values of CNT: MV-350 nanocomposites and individual components.

	CNT	MV-350	CNT:MV-350 (80:20)[a]	CNT:MV-350 (50:50) [a]	CNT:MV-350 (20:80) [a]
Csp ($F.g^{-1}$)	2.0	4.4 E^{-03}	4.01	3.8	1.7

[a] Percentage by mass

A synergistic effect between the carbon material and biosilica was observed in all the tested composites. The capacitance performance of nanocomposites containing at least 50 % of CNT was almost two-fold higher than that of pure CNT and nine hundred-fold higher than that of the diatom-derived solid.

Table 6. Specific capacitance values of CNT:MV (80:20) nanocomposites at different pyrolysis temperatures

	CNT: MV-300	CNT: MV-350	CNT: MV-400	CNT: MV-450	CNT: MV-500	CNT: MV-600	CNT: MV-700
Csp ($F.g^{-1}$)	4.42	4.01	2.80	3.07	2.97	2.33	2.65

In Table 6 it can be seen that even when the carbon content in the samples pyrolyzed at elevated temperatures is almost zero, the specific capacitance is still higher than for the separate elements. This improved capacitance behavior could also be ascribed to an appropriate pore texture, increased surface area (see Figure 7) and high electrical conductivity of the carbon component that favors fast ionic diffusion. In addition, a good interaction between carbonaceous and silica structures resulted in a material with a better capacitance performance, which is a promising result for the preparation of further composites.

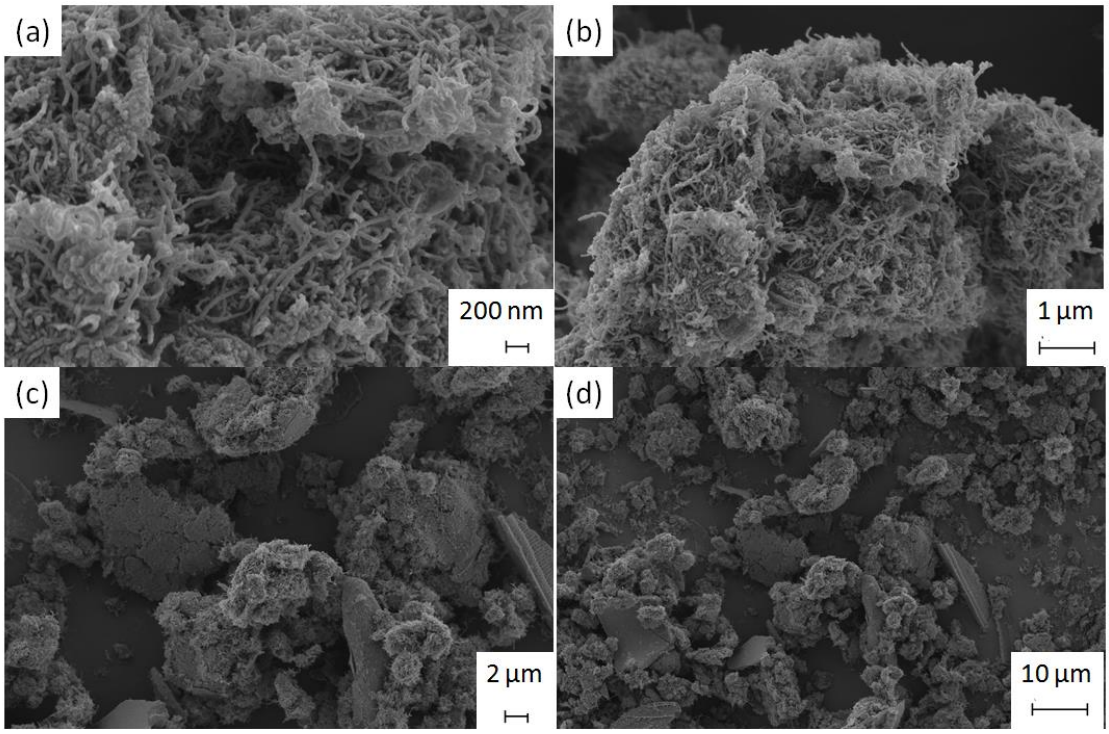

Figure 8. SEM micrographs of CNT:MV-350 (80:20) nanocomposites at different magnifications.

Conclusions

Fast pyrolysis studies of diatom *Melosira varians* (MW) were conducted between 300 and 700 °C to investigate the influence of pyrolysis temperature on product yields. A predominance of the solid fraction was obtained at all the temperatures (59-88 % yield). The largest production of bio-oil was accomplished at 450 °C (29 % yield), when palmitic acid was formed in considerable amounts. High concentrations of fatty acids add considerable value to the bio-oil as potential fuel, which must nevertheless be upgraded to further improve these features.

The solid materials derived from MV pyrolysis were exhaustively characterized and showed an amorphous silica structure which remained practically unaffected by the different pyrolysis conditions. The BET surface area of these materials was very low (12-21 $m^2.g^{-1}$), although in the SEM micrographs the frustules have micrometric and nanometric pores.

Cyclic voltammetry experiments were performed to evaluate the capacitance properties of the diatom-derived solids. The specific capacitance values of these siliceous solids were very low. More importantly, the electrochemical evaluation of a composite formed by carbon nanotubes and the solid obtained at 350 ºC led to a great improvement in the conductivity of the material. The synergistic effect could be attributed to the increased surface area exposed to the electrolyte due to CNT and other effects promoted by the presence of the biosilica structure, which should be studied in further depth in future research.

Acknowledgements

Thanks are due for the financial support provided by National Research Council of Argentina (CONICET) and Secretariat of Science and Technology (SECyT) from National University of Córdoba. R.V.P. thanks CIN for her fellowship. LAMARX is gratefully acknowledged for the use of the SEM-EDS and Ing. Julio Daniel Fernández (UTN) for BET measurements.

References

1. Czernik, S., Bridgwater, A., , *Overview of applications of biomass fast pyrolysis oil.* Energy Fuels, 2004. **18**: p. 590-598.
2. Miao, X., Wu, Q. and Yang, C., *Fast pyrolysis of microalgae to produce renewable fuels.* Journal of Analytical and Applied Pyrolysis, 2004. **71**: p. 855-863.
3. Dalagan, J.Q.E., E. P., *Interaction of diatom silica with graphene.* Philippine Science Letters, 2013. **6**(1).
4. Yuan, R.-H.J.J.-J., *Learning from Biosilica: Nanostructured Silicas and their coatings on substrates by programmable approaches.* Advances in Biomimetics, 2011: p. 159-184.
5. Losic, D.Y., Y.; Aw, M. S.; Simovic, S.; Thierry, B.; Addai-Mensah, J., *Surface functionalisation of diatoms with dopamine modified iron-oxide nanoparticles: toward magnetically guided drug microcarriers with biologically derived morphologies.* ChemComm, 2010. **46**: p. 6323-6325.
6. Qian, T.L., J.; Min, X.; Deng, Y.; Guan, W.; Ning, L., *Diatomite: A promising natural candidate as carrier material for low, middle and high temperature phase change material.* Energy Conversion and Management, 2015. **98**: p. 34-45.
7. Konuklu, Y.E., O.; Gokce, O., *Easy and industrially applicable impregnation process for preparation of diatomite-based phase change material nanocomposites for thermal energy storage.* Applied Thermal Engineering, 2015. **91**: p. 759-766.
8. Das, V.K.T., A. J., *Greener oxidation of aldehydes over bio-silica supported Fe2O3 nanoparticles: A convenient "NOSE" approach.* Applied Catalysis A: General, 2014. **470**: p. 97-103.
9. Wen-Tien Tsai, C.-W.L., Kuo-Jong Hsien, *Characterization and adsorption properties of diatomaceous earth modified by hydrofluoric acid etching.* Journal of Colloid and Interfase Science, 2006. **297**: p. 749-754.
10. Bakr, H.E.G.M.M., *Diatomite: Its characterization, modifications and applications.* Asian Journal of Materials Science, 2010. **2**(3): p. 121-136.
11. Meradi, H.A., L.; Bahloul, L.; Labiod, K.; Ismail, F., *Contribution to characterization of the diatomite for industrial application.* Energy Procedia, 2015. **In press**.
12. Bridgwater, A.V., *Biomass fast pyrolysis.* Thermal Science, 2004. **8**(2): p. 21-49.
13. Lopez, G.A., R.; Olazar, M.; Arabiorrutia, M.; Bilbao, J., *Kinetics of scrap tyre pyrolysis under vacuum conditions.* Waste Management, 2009. **29**(10): p. 2649-2655.
14. Wang, S.W., Q.; Jiang, X.; Han, X.; Ji, H., *Compositional analysis of bio-oil derived from pyrolysis of seaweed.* Energy Conversion and Management, 2013. **68**: p. 273-280.

15. Kan, T., Grierson, S., de Nys, R., Strezov, V., *Comparative Assessment of the Thermochemical Conversion of Freshwater and Marine Micro- and Macroalgae.* Energy and Fuels, 2014. **28**: p. 104-114.
16. Liang, Y., *Producing liquid transportation fuels from heterotrophic microalgae.* Applied Energy, 2013. **104**: p. 860-868.
17. Hu, Z., Zheng, Y., Yan, F., Xiao, B., Liu, S., *Bio-oil production through pyrolysis of blue-green algae blooms (BGAB): Product distribution and bio-oil characterization.* Energy, 2013. **52**: p. 119-125.
18. Bailliez, V.O., A.; Cleophax, J., *Sinthesis of polynitrogenated analogues of glucopyranoses from levoglucosan.* Tetrahedron, 2004. **60**: p. 1079-1085.
19. Simoneit, B.S., J.; Nolte, C.; Oros, D.; Elias, V.; Fraser, M.; Rogger, W.; Cass, R., *Levoglucosan, a tracer for cellulose in biomass burning and atmospheric particles.* Atmospheric Environment, 1999. **33**: p. 173-182.
20. Yamanaka, S.Y., R.; Usami, H.; Hayashida, N.; Ohguchi, M.; Takeda, H.; Yoshino, K., *Optical properties of diatom silica frustule with special reference to blue light.* Journal of Applied Physics, 2008. **103**.
21. Fowler, C.E.B., C.; Lebeau, B.; Patarin, J.; Delacote, C.; Walcarius, A., *An aqueous route to organically functionalized silica diatom skeletons.* Applied Surface Science, 2007. **253**: p. 5485-5493.
22. Carrier, M.J., J. E.; Danje, S.; Hugo, T.; Gorgens, J.; Knoetze, J. H., *Impact of the lignocellulosic material on fast pyrolysis yields and product quality.* Bioresource Technology, 2013. **150**: p. 129-138.
23. Bleda-Martínez, M.J.P., J. M.; Linares-Solano, A.; Morallón, E.; Cazorla-Amorós, D., *Effect of surface chemistry on electrochemical storage of hydrogen in porous carbon materials.* Carbon, 2008. **46**(7): p. 1053-1059.
24. Vieira, M.G.A.d.A.N., A. F.; da Silva, M. G. C.; Nóbrega, C. C.; Melo Filho, A. A., *Characterization and use of in natura and calcined rice husks for biosorption of heavy metals ions from aqueous effluents.* Brazilian Journal of Chemical Engineering, 2012. **29**(3): p. 619-633.
25. Chaisena, A.R., K.;, *Effects of thermal and acid treatments on some physico-chemical properties of lampang diatomite.* Suranaree Journal of Science and Technology, 2014. **11**: p. 289-299.
26. Gulturk, E.G., M., *Thermal and acid treatment of diatom frustules.* Journal of Achievements in Materials and Manufacturing Engineering, 2011. **46**(2): p. 196-203.
27. Kow, K.W.Y., R.; Abdul Aziz, A. R.; Abdullah, E. C., *Characterization of bio-silica synthesised from cogon grass (Imperata cylindrica).* Power Technology, 2014. **254**: p. 206-213.
28. Jantschke, A.K., E.; Mance, D.; Weingarth, M.; Brunner, E.; Baldus, M., *Insight into the supramolecular architecture of intact diatom biosilica from DNP-Supported Solid-State NMR Spectroscopy.* Angewandte Chemie, 2015. **54**: p. 1-6.
29. Bao, Z.W., M. R.; Shian, S.; Cai, Y.; Graham, P. D.; Allan, S. M.; Ahmad, G.; Dickerson, M. B.; Church, B. C.; Kang, Z.; Abernathy III, H. W.; Summers, C. J.; Liu, M.; Sandhage, K. H., *Chemical reduction of three-dimensional silica micro-assemblies into microporous silicon replicas.* Nature, 2007. **446**: p. 172-175.
30. Adinaveen, T., John Kennedy, L. J., Vijaya, J. J., Sekaran, G., *Studies on structural, morphological, electrical and electrochemical properties of activated carbon prepared from sugarcane bagasse.* Journal of Industrial and Engineering Chemistry, 2013. **19**: p. 1470-1476.
31. Pintor, M.J.J.-M., C.; Jeanne-Rose, V.; Taberna, P. T.; Simon, P.; Gamby, J.; Gadiou, R.; Gaspard, S., *Preparation of activated carbon from Turbinaria turbinata seaweeds and its use as supercapacitor electrode materials.* Comptes Rendus Chimie, 2013. **16**: p. 73-79.

32. Gao, X.X., W.; Zhou, J.; Wang, G.; Zhuo, S.; Liu, Z.; Xue, Q.; Yan, Z., *Superior capacitive performance of active carbons derived from Enteromorpha prolifera.* Electrochimica Acta, 2014. **133**: p. 459-466.
33. Kalyani, P. and A. Anitha, *Biomass carbon & its prospects in electrochemical energy systems.* International Journal of Hydrogen Energy, 2013. **38**(10): p. 4034-4045.
34. Yu, D., Dai, L., *Self-Assembled graphene/carbon nanotube hybrid films for supercapacitors.* The Journal of Physical Chemestry Letters, 2010. **1**: p. 467-470.
35. Zeng, F., Kuang, Y., Zhang, N., Huang, Z., Pan, Y., Hou, Z., Zhou, H., Yan, C., Schmidt, O. G., *Multilayer super-short carbon nanotube/reduced graphene oxide architecture for enhanced supercapacitor properties.* Journal of Power Sources, 2014. **247**: p. 396-401.
36. Tan, X.F.L., Y. G.; Gu, Y. L.; Xu, Y.; Zeng, G. M.; Hu, X. J.; Liu, S. B.; Wang, X.; Liu, S. M.; Li, J., *Biochar-based nano-composites for the decontamination of wastewater: A review.* Bioresource Technology, 2016. **212**: p. 318-333.